JOURNAL OF
APPLIED
CRYSTALLOGRAPHY

Volume 55 (2022)

Supporting information for article:

Molecular dynamics investigation of a one-component model for the stacking motif in complex alloy structures

Jung Wen Yeh, Kouji Tomita, Yuuta Imanari and Masaya Uchida

Supporting Information: Molecular dynamics investigation of a one-component model for the stacking motif in complex alloy structures

Jung Wen Yeh[a], Kouji Tomita[b], Yuuta Imanari[b] and Masaya Uchida[ac]*

[a]Department of Information Systems, Graduate School of Engineering, Saitama Institute of Technology, Fukaya, Saitama, 369-0293, Japan

[b]Department of Information Systems, Faculty of Engineering, Saitama Institute of Technology, Fukaya, Saitama, 369-0293, Japan

[c]Advanced Science Research Laboratory, Saitama Institute of Technology, Fukaya, Saitama, 369-0293, Japan

Correspondence email: uchida.masaya@sit.ac.jp

1. Time-averaged atomic positions

Time-averaged atomic positions were obtained from the trajectory of the molecular dynamics (MD) simulations for the μ-Al_4Mn phase; these time-averaged positions are given in Table S1.

Table S1. Time-averaged atomic positions of the Al atoms. The data is in units of Å on a three-dimensional Cartesian coordinate system. The configurations are obtained 190 ps after relaxation (see Fig. 3). The A-layer is set to be at $z = 0$. The resulting atomic arrangement indicates a pseudo-mirror symmetry about the A-layer within standard deviation.

	x	y	z
1	2.5	0	0
2	10	0	0
3	17.5	0	0
4	-1.25	2.165	0
5	1.25	2.165	0
6	3.75	2.165	0
7	6.25	2.165	0
8	8.75	2.165	0
9	11.25	2.165	0
10	13.75	2.165	0
11	16.25	2.165	0
12	0	4.33	0
13	5	4.33	0
14	7.5	4.33	0
15	12.5	4.33	0
16	15	4.33	0
17	-1.25	6.495	0
18	1.25	6.495	0
19	6.25	6.495	0
20	13.75	6.495	0
21	-5	8.66	0
22	-2.5	8.66	0
23	0	8.66	0
24	2.5	8.66	0
25	5	8.66	0
26	7.5	8.66	0
27	10	8.66	0
28	12.5	8.66	0
29	-3.75	10.825	0
30	3.75	10.825	0
31	8.75	10.825	0
32	11.25	10.825	0
33	-5	12.99	0
34	-2.5	12.99	0
35	2.5	12.99	0
36	5	12.99	0
37	10	12.99	0
38	-8.75	15.155	0
39	-6.25	15.155	0
40	-3.75	15.155	0
41	-1.25	15.155	0
42	1.25	15.155	0
43	3.75	15.155	0
44	6.25	15.155	0
45	8.75	15.155	0
46	0.10±0.14	2.72±0.16	-2.50±0.10
47	2.44±0.11	1.33±0.12	-2.52±0.13
48	4.93±0.09	0.01±0.11	-1.46±0.16
49	7.59±0.12	2.73±0.24	-2.44±0.09
50	15.12±0.09	-0.03±0.06	-1.54±0.13
51	17.61±0.16	1.46±0.12	-2.49±0.07
52	20.08±0.21	5.55±0.16	-2.43±0.12
53	0.03±0.30	-0.06±0.22	-3.85±0.13
54	4.83±0.14	2.80±0.15	-2.39±0.09
55	11.37±0.08	6.57±0.10	-1.47±0.15
56	8.63±0.10	6.56±0.11	1.50±0.18
57	10.00±0.11	1.36±0.16	-2.48±0.13
58	12.37±0.13	2.78±0.16	-2.44±0.10
59	17.58±0.13	4.21±0.10	-1.56±0.10
60	3.79±0.12	9.34±0.14	-2.43±0.08
61	2.43±0.13	4.16±0.11	-1.52±0.14
62	6.31±0.22	5.16±0.12	-2.46±0.12
63	8.59±0.13	9.34±0.14	-2.45±0.09
64	11.40±0.14	9.31±0.13	2.44±0.09
65	16.21±0.09	6.57±0.10	-1.49±0.15
66	13.75±0.16	5.17±0.10	-2.42±0.07
67	-4.89±0.16	2.68±0.16	-2.45±0.09
68	1.36±0.15	7.99±0.14	-2.43±0.08
69	1.35±0.10	10.77±0.13	-1.48±0.15
70	3.79±0.15	6.51±0.09	-1.47±0.14
71	6.17±0.13	7.96±0.11	-2.43±0.07
72	13.84±0.11	10.75±0.12	-1.44±0.15
73	11.39±0.15	9.41±0.23	-2.43±0.10
74	-3.81±0.12	9.39±0.17	-2.46±0.11
75	-1.45±0.11	7.91±0.19	-2.46±0.10
76	-0.01±0.11	13.13±0.10	-1.44±0.21
77	5.22±0.17	14.50±0.13	-2.43±0.09
78	6.19±0.10	10.75±0.11	-1.48±0.12
79	13.75±0.16	7.99±0.11	-2.46±0.10
80	12.47±0.14	13.08±0.14	-1.45±0.14
81	-3.95±0.40	12.31±0.50	-2.43±0.10
82	-1.40±0.15	10.74±0.13	-1.56±0.14
83	0.00±0.15	15.86±0.14	-2.48±0.10
84	2.40±0.09	17.34±0.08	-1.47±0.12
85	3.79±0.27	12.14±0.12	-2.42±0.11
86	7.60±0.13	13.08±0.12	-1.49±0.16
87	10.00±0.22	11.76±0.13	-2.41±0.10
88	-9.98±0.06	17.32±0.10	-1.30±0.09
89	-7.59±0.18	15.91±0.11	-2.46±0.08
90	-2.40±0.09	17.32±0.10	-1.48±0.12
91	-2.49±0.20	14.53±0.15	-2.41±0.10
92	2.44±0.15	14.54±0.19	-2.46±0.11
93	7.61±0.14	15.93±0.14	-2.47±0.13
94	10.00±0.15	14.58±0.13	-2.49±0.12
95	-2.40±0.11	1.47±0.10	2.43±0.10
96	4.87±0.13	2.78±0.24	2.46±0.09
97	2.46±0.11	1.44±0.10	2.47±0.14
98	10.03±0.11	1.43±0.13	2.45±0.11
99	8.62±0.14	6.57±0.11	-1.49±0.14
100	12.40±0.10	-0.02±0.09	1.48±0.13
101	15.11±0.10	0.00±0.12	1.49±0.14
102	-1.37±0.14	8.03±0.21	2.46±0.08
103	2.41±0.10	4.22±0.09	1.48±0.17
104	6.19±0.25	5.12±0.13	2.47±0.11
105	9.94±0.15	4.19±0.11	-1.47±0.14
106	11.41±0.13	6.56±0.15	1.50±0.15
107	15.22±0.16	2.84±0.13	2.44±0.08
108	17.61±0.11	4.27±0.11	1.44±0.14
109	-0.09±0.11	5.61±0.15	2.45±0.10
110	0.01±0.12	2.82±0.14	2.45±0.11
111	3.78±0.13	6.57±0.12	1.51±0.14
112	9.96±0.20	11.73±0.11	2.46±0.07
113	7.62±0.14	2.76±0.22	2.45±0.08
114	12.47±0.13	2.77±0.21	2.44±0.09
115	16.22±0.11	6.62±0.10	1.47±0.10
116	-3.79±0.13	9.40±0.11	2.45±0.08
117	0.01±0.13	13.12±0.15	1.50±0.19
118	3.86±0.15	12.13±0.11	2.41±0.08
119	1.38±0.12	7.96±0.25	2.45±0.12
120	6.17±0.13	7.95±0.11	2.43±0.08
121	10.01±0.10	4.17±0.13	1.46±0.16
122	13.78±0.07	10.78±0.08	1.50±0.14
123	-3.78±0.19	12.19±0.10	2.43±0.12
124	-2.43±0.13	17.32±0.11	1.46±0.14
125	1.39±0.12	10.78±0.11	1.48±0.16
126	3.78±0.09	9.39±0.11	2.47±0.10
127	6.25±0.12	10.77±0.09	1.54±0.10
128	10.00±0.12	14.52±0.11	2.43±0.09
129	8.60±0.16	9.37±0.17	2.45±0.10
130	-7.60±0.11	13.12±0.12	1.52±0.12
131	-7.61±0.15	15.97±0.14	2.43±0.08
132	-2.41±0.13	14.51±0.13	2.43±0.11
133	-1.38±0.11	10.77±0.11	1.51±0.16
134	2.39±0.12	14.50±0.17	2.44±0.09
135	7.58±0.12	13.13±0.09	1.54±0.13
136	13.80±0.12	7.98±0.16	2.46±0.09
137	-10.02±0.10	17.33±0.10	1.54±0.11
138	-5.12±0.10	17.33±0.11	1.49±0.11
139	-5.21±0.14	14.54±0.15	2.46±0.12
140	-0.05±0.11	15.92±0.15	2.45±0.11
141	5.15±0.08	14.51±0.15	2.41±0.07
142	3.77±0.20	22.50±0.15	2.47±0.11
143	7.55±0.12	15.99±0.13	2.42±0.10

2. MD simulations in the cases of Cu, Pd, Ni, and Ag

We also performed similar MD simulations by replacing Al (as presented in the main paper) from μ-Al_4Mn with Cu, Pd, Ni, and Ag. We used the embedded atom method potentials for Cu–Cu (Cu_smf7.eam; Foiles, 1985), Pd–Pd (Pd_u3.eam; Foiles *et al.*, 1986), Ni–Ni (Ni_smf7.eam; Foiles, 1985), and Ag–Ag (Ag_u3.eam; Foiles *et al.*, 1986). Figures S1–S4 show typical snapshots of the arrangement for Cu, Pd, Ni, and Ag atoms adsorbed on the A-layer [see Fig. 3].

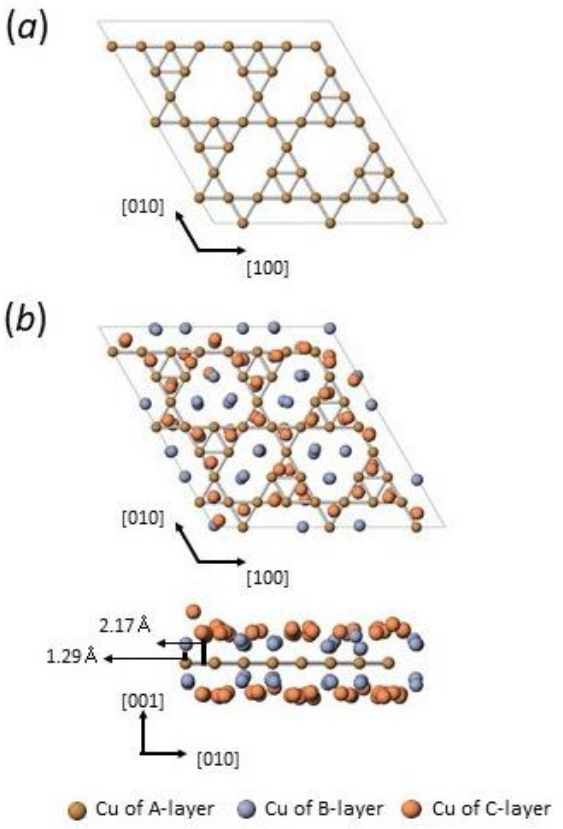

Figure S1. (a) Ball-and-stick view of a close-packed layer of Cu (the A-layer) with atomic vacancies perpendicular to the [001] axis; the configuration depicts data obtained from MD simulations at 800 K (an $8a_0 \times 8a_0$ hexagonal cell with $a_0 = 2.3$ Å). The reddish-brown circles represent Cu atoms in the A-layer. (b) Snapshot of the arrangement of Cu atoms adsorbed on the A-layer after relaxation; the configuration was obtained from a MD simulation at 800 K. The blue and orange circles represent Cu atoms in the B- and C-layers, respectively. All the added atoms were adsorbed onto the A-layer. The different colors represent atoms in different positions along the [001] direction.

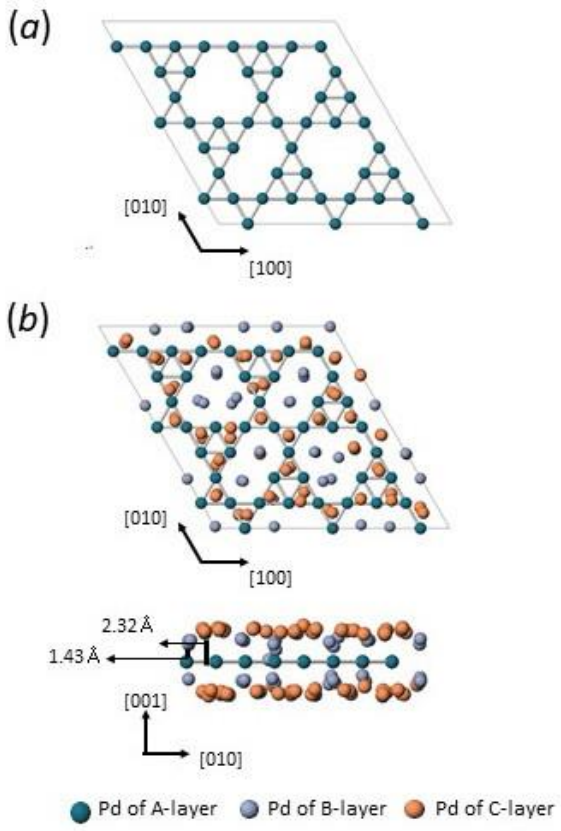

Figure S2. (a) Ball-and-stick view of a close-packed layer of Pd (the A-layer) with atomic vacancies perpendicular to the [001] axis; the configuration depicts data obtained from MD simulations at 1000 K (an $8a_0 \times 8a_0$ hexagonal cell with $a_0 = 2.5$ Å). The blue–green circles represent Pd atoms in the A-layer. (b) Snapshot of the arrangement of Pd atoms adsorbed on the A-layer after relaxation; the configuration was obtained from MD simulations at 800 K. The blue and orange circles represent Pd atoms in the B- and C-layers, respectively. All the added atoms were adsorbed onto the A-layer. The different colors represent atoms in different positions along the [001] direction.

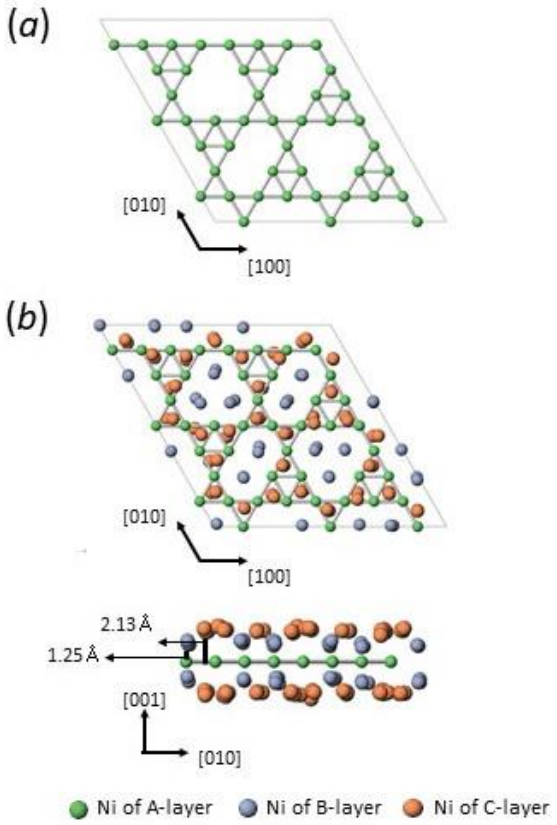

Figure S3. (a) Ball-and-stick view of a close-packed layer of Ni (the A-layer) with atomic vacancies perpendicular to the [001] axis; the configuration depicts data obtained from MD simulations at 1000 K (an $8a_0 \times 8a_0$ hexagonal cell with $a_0 = 2.3$ Å). The light-green circles represent Ni atoms in the A-layer. (b) Snapshot of the arrangement of Ni atoms adsorbed on the A-layer after relaxation; the configuration was obtained from MD simulations at 1100 K. The blue and orange circles represent Ni atoms in the B- and C-layers, respectively. All the added atoms were adsorbed onto the A-layer. The different colors represent atoms in different positions along the [001] direction.

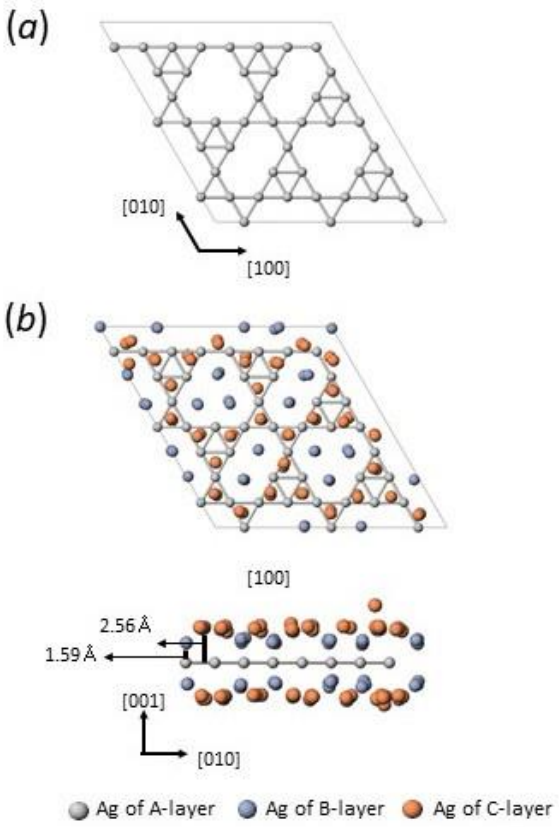

Figure S4. (a) Ball-and-stick view of a close-packed layer of Ag (the A-layer) with atomic vacancies perpendicular to the [001] axis; the configuration depicts data obtained from MD simulations at 700 K (an $8a_0 \times 8a_0$ hexagonal cell with $a_0 = 2.5$ Å). The silver-grey circles represent Ag atoms in the A-layer. (b) Snapshot of the arrangement of Ag atoms adsorbed on the A-layer after relaxation; the configuration was obtained from MD simulations at 800 K. The blue and orange circles represent Ag atoms in the B- and C-layers, respectively. All the added atoms were adsorbed onto the A-layer. The different colors represent atoms in different positions along the [001] direction.

References

Foiles, S. M. (1985). *Phys. Rev.* B **32**, 7685–7693.
Foiles, S. M., Baskes, M. I. & Daw, M. S. (1986). *Phys. Rev.* B **33**, 7983–7991.